CHAPTER FOUR: RESULTS AND DISCUSSION

4.1 Formation of copper dots on oxidized wafer surface

Growing of copper dots on wafer surface involves of (i) dissolving copper atoms from anode into methanol, (ii) transportation of copper ions from anode to cathode, (iii) generation of localized conducting paths at oxide layer and (iv) deposition of copper ions on these localized conducting paths. The above items are studied and discussed in this section.

4.1.1 Analyzing the purity of anode using Energy Dispersive X-ray Spectroscopy (EDS)

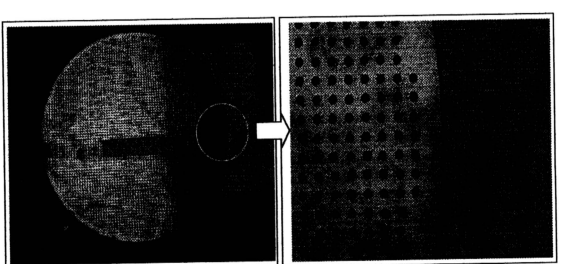

Figure 4.1: The anode of the copper decoration unit is a copper mesh with thousand of holes (≈ 2 mm in diameter).

Anode uses in copper decoration technique is a copper mesh as shown in Fig. 4.1. It is made of high purity copper. This is because no other metallic element can be found, except copper element by using Energy - Dispersive X-ray (EDS) analysis on the copper plate. The result of EDS analysis is given in Fig. 4.2.

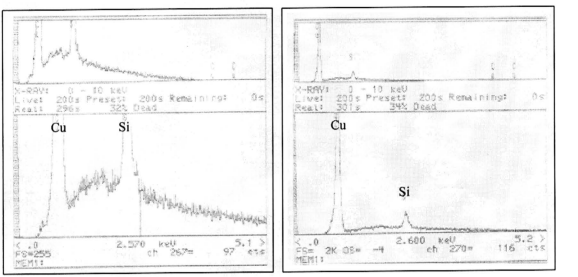

Figure 4.2: EDS analysis on the copper plate shows that the anode is made of highly pure copper material. No other metallic element is detected except copper element.

Anode plays two important roles in the decoration process. Since it is connected to the positive terminal of power supply, it becomes one of the terminals to supply electric field that uses to stress the oxide layer. Anode also acts as the source of copper ions. The copper atoms of anode release their valence electrons and dissolve in the methanol as copper ions.

$$Cu(s) \longrightarrow Cu^{2+}(ac) + 2e^{-} \qquad (15)$$

The effect of copper atoms dissolving from anode contributes to wear off of copper plate as a function of usage time. The copper plate gets thinner and holes on the plate get larger as illustrated in Fig. 4.3. The weight of the plate is reduced too. The other factor that also can wear off the copper plate is the cleaning of copper decoration unit in the beginning of each copper decoration process. This is because diluted nitric acid (≈ 1% vol.) is applied to remove copper oxide especially from the copper plate.

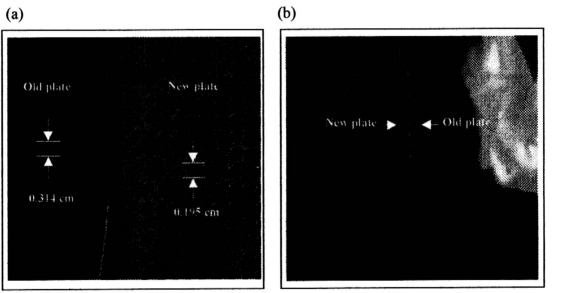

Figure 4.3: (a) The old plate has larger holes (d: 0.314 cm) compared to new plate (d: 0.195 cm). (b) The thickness of new plate is larger (0.292 cm) compared to old plate (0.173 cm). The copper plate wears off as a function of usage time. This is because the copper atoms receive electrons and dissolve into the methanol as copper ions during decoration process.

4.1.2 Determination of copper concentration in methanol using ICP-OES

Since copper atoms are injected into methanol during decoration process, the copper concentration in methanol is expected to build up with time. This can be verified by measuring copper concentration in methanol periodically over time using ICP-OES. The experimental result measured by ICP-OES is illustrated in Fig. 4.4 (b) (curve E1).

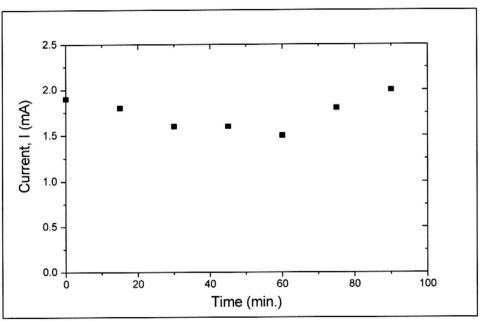

Figure 4.4 (a): The current fluctuates during the seasoning period. To simplify the calculation of copper concentration in methanol, the average current of 0.0017A is taken in this estimation.

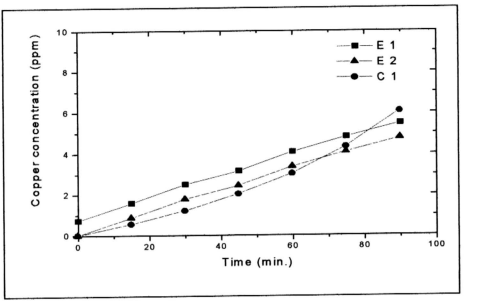

Figure 4.4 (b): The copper concentration in methanol measures using ICP-OES shows that the copper concentration increases as a function of decoration period (curve E 1). Curve E 2 is the copper concentration level in the methanol after subtracting the residual copper in the methanol at t = 0. Based on the current, decoration time and volume of methanol, the calculated copper concentration is plotted (curve C1) as a function of time. Although the calculated copper concentration in methanol (C 1) is lower compared to E 2 (C1 is expected to be higher than E 2), both the lines are in same order of magnitude. The increasing rate of copper concentration (slope of E1) is 0.053 (ppm/ min.).

The copper concentration in methanol is found to increase linearly as a function of decoration time.

The theoretical copper concentration in methanol is calculated (Appendix A) based on the electrical current (I), decoration time (t) and volume of methanol (V_f). The volume of methanol (V_f) is decreasing with time mainly due to evaporation to surrounding. It is difficult to determine V_f at each time interval (e.g. 15, 30, ..., 90 minutes.) practically. Therefore, V_f is assumed to be a linear function

in the calculation. This derivation is ended with equation *(16)*, where the calculated copper concentration is not only a linear function of time, but also depends on the reciprocal of the volume of methanol (V_t) at time, t.

$$\left[Cu^{2+}\right] = 5.6\text{x}10^{-7}\left(\frac{t}{V_t}\right) ppma \qquad (16)$$

As shown in Fig. 4.4 (b), the calculated copper concentration (curve C1) is in the same order of magnitude as compared with the experimental result (curve E2). This shows that the copper concentration in the methanol depends on the decoration time. Nevertheless, the calculated value is expected to be higher than the experimental value at all time. This is because the calculated value does not include copper atoms deposited on the wafer surface. The amount of copper measured with ICP-OES therefore should be less than the calculated copper concentration.

One of the possible reasons that C1 is lower than E2 might be due to overestimate the volume of methanol V_t at time t. The volume of methanol might decrease exponentially rather than linearly. However, the volume of methanol at time t is difficult to measure practically.

The effect of the magnitude of the current flows through the copper decoration equipment on the copper concentration is also studied. Fig. 4.5 shows that the larger the magnitude of current flows, more copper atoms is dissolved into the methanol.

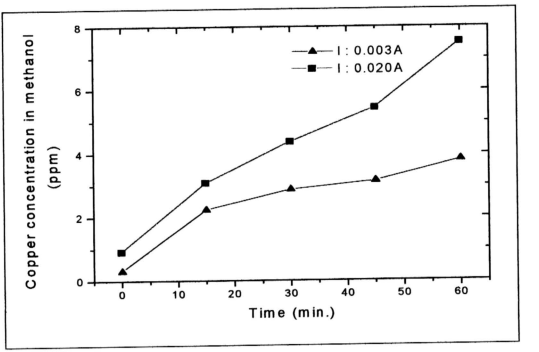

Figure 4.5: Larger magnitude of current during copper decoration resulting higher copper decoration in methanol. This indicates that the copper concentration in methanol is also current dependent.

4.1.3 Copper ions transportation in methanol

Copper ions that dissolved into the methanol are positively charged. Majority of these copper ions is distributed in the gap between anode and cathode. The existence of a gap requires copper ions that dissolved from anode to travel through the methanol before being discharged and deposited on the oxide surface. In electrolysis process, ions can be traveled through diffusion, convection and migration [17]. However, in the case of copper decoration, ions are transported to the surface of oxide layer mainly by migration and diffusion mechanism. The transportation of charge carriers is not by convection. This is because convection involves of mechanical transport of ions or molecules through a solution as a result of stirring, vibration, or temperature gradient. However, in copper decoration process, there is no stirring, vibration or temperature gradient.

In migration, ions will move under the influence of an electric field. The potential gradient between the anode and the oxide layer (V_{drop}), serves to drive the copper ions to the oxide surface [5]. This potential gradient (V_{drop}) decreases with copper concentration in methanol. Change of V_{drop} with copper concentration in methanol will be discussed in more details in section 4.3.1.

4.1.4 Detection of permanent damages extended to wafer surface as a result of oxide breakdown

Since oxidized wafer is placed on top of the plate that connected to negative terminal of DC power supply, it becomes the cathode as depicted in Fig. 2.1 (a). SiO_2 layer of the wafer is an insulator. It should not allow electrical current to flow through during copper decoration. Therefore, no cation should deposit on the oxide surface. However, in practice, thousand of copper dots are grown on the wafer surface as shown in Fig. 2.2 (a) (i) and (ii). This indicates that there are thousand of localized conducting paths generated through the oxide layer during copper decoration process. Or else, copper dots will not be able to form on wafer surface because no supply of electrons for deposition of cations.

As discussed in section 2.2.2 also, the conducting paths are generated by high thermal energy dissipated during oxide breakdown. This energy is great enough to cause chemical changes and bond breaking especially on the oxide film. These low resistance paths allow current to flow through the oxide layer and supply electrons required for discharging the cations.

In this report, the author would like to point out that damages are created not only in the oxide but extended on the wafer surface during the copper decoration process. Preferential etching can be used to reveal or enlarge these damages in order to observe under low optical microscope. Damages induced on the surface of the wafer due to oxide breakdown are shown in Fig. 4.6 (a), (b), (c) and (d).

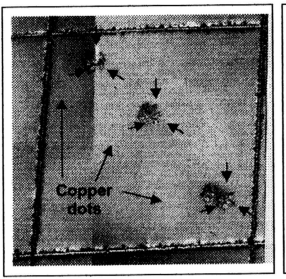

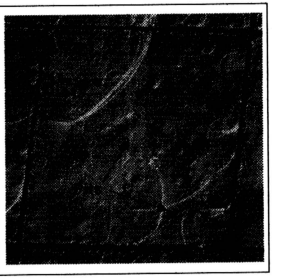

(a) (b)

Figure 4.6: (a) Three copper dots are found in this grid. (b) After preferential etching, small etching pits are found located under the copper dots. We believe that the pit is due to damages created on the surface of the wafer during copper decoration process. The damaged site is enlarged because undergoes faster etching rate during preferential etching.

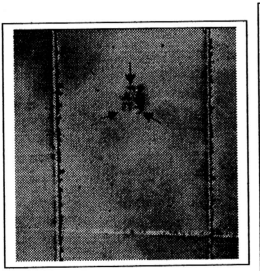

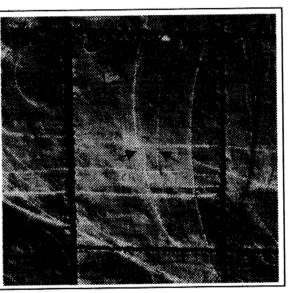

(c) (d)

Figure 4.6: (c) Another rectangular box with copper dot. (d) Pit is found exactly underneath the copper dot after preferential etching. A high resolution image of this pit which captured by AFM is shown in Fig. 4.6 (e).

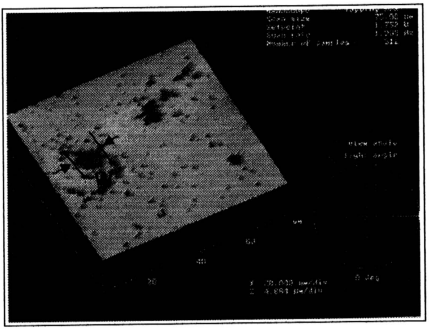

Figure 4.6: (e) Pits are found on the wafer surface. The width and depth of one of the pits is 17.9 μm and 65 nm, respectively. The AFM scanning size is 75 μm and the scanning rate is 2Hz.

Flow pattern defects (FPDs), which have circular patterns, can be clearly seen on the preferential etched wafer's surface. The origin of FPDs is crystal grown in defects. Beside FPDs, pits are also found located right underneath some of the copper dots. This provides evidence to show that after oxide breakdown, permanent damages are created not only in the oxide layer but extends to the wafer surface. These physical damages are created due to the energy dissipated by the injected electrons. As a result, after the oxide layer is removed and the wafer is preferentially etched, the damaged sites experience a faster etching rate compared to other regions. This results in formation of pits. The above explanation is simplified in Fig. 4.7. The dimension of one of the pits is found to have a width of 17.9 μm and a depth of 65 nm as given in Fig. 4.6 (e).

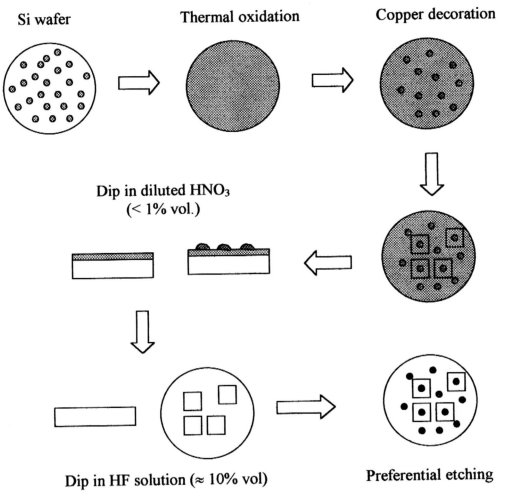

Figure 4.7: Silicon wafer consists of grown in defects such as D-defects. After thermal oxidation, these defects are integrated into the oxide layer. When the wafer is copper decorated, copper dots are formed on top of these defects. Due to oxide breakdown, damages not only created through the oxide layer, but also extended to the wafer surface. Following on this, rectangular boxes are drawn on the wafer surface to register the location of the copper dots. Then, copper dots and oxide layer is removed by diluted nitric acid and HF solution, respectively. The damages on the wafer surface cannot be seen at this stage. However, preferential etching can reveal them. As a result, these damages can be observed under a microscope at low magnification (50X) as etching pits.

Pits found on wafer surface after Secco etching indicates that damages are created during copper decoration not only at oxide layer but extends on wafer surface.

4.1.5 Studying distribution of copper dots size on copper decorated wafers

It is believed that different degree of damage is created at the oxide layer during oxide breakdown. One of the possible observations is through the magnitude of current flowing through the breakdown spots when the oxide layer is stressed with constant voltage. Higher magnitude of current should flow through the breakdown paths that experienced more severe damages. This phenomenon is observed in GOI measurement [9]. In the case of copper decoration technique, one should observe differences in the size of copper dots on a piece of copper decorated wafer. This is because the amount of electrons (current) that used to deposit copper ions at different breakdown spot is different within each other.

Fig. 4.8 (a) and (b) illustrates the results of size distribution inspected on 2 pieces of copper decorated wafers. The number of copper dots measured is around 10% of the total dots on each piece of wafers.

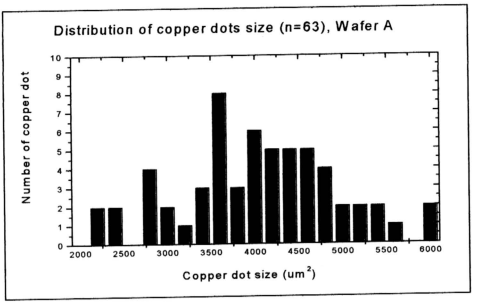

Figure 4.8: (a) The number of copper dots measured is around 6.3% from the total number of copper dot over the wafer surface. It is found that the size of copper dots is distributed over a wide range, starts from 2000 to 6000 μm^2 for wafer A. Since the decoration time is constant and the amount of copper ions discharged (size of copper dot) depends on the total charges supplied to the breakdown spots, the magnitude of current flows through the spots must be different at each breakdown spots.

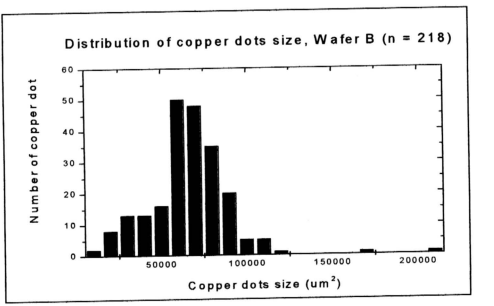

Figure 4.8: (b) Similar observation is obtained in wafer B. The size of copper dots is distributed over a wide range, i.e. from 10,000 to 20,000 μm^2. The number of copper dots measured is around 11.3% over the total copper dots on the wafer surface.

The average size of copper dots is different for these 2 pieces of wafers. This is attributed to the difference of copper concentration in methanol during the decoration process. Since formation of copper dots is due to electrolysis process, differences in copper dots size on the same piece of wafer is due to the total charges supplied to the breakdown spots for discharging the copper ions. In this case, the wafers are decorated with the same time period. Therefore, the difference in the total amount of charges is due to the difference in the magnitude of current flowing through the breakdown spots. This indicates that damages created on the oxide during oxide breakdown are not the same over the whole oxide layer. This phenomenon is most likely due to the oxide defects that induced different degree of weak spots in the oxide film. Consequently, when a constant voltage/field is applied to the oxide layer, the weaker spots experience more damages during oxide breakdown and allow larger current to flow through them. This hypothesis will be further studied in section 4.1.6 and 4.1.7.

4.1.6 Studying the impact of size of D-defect on the size of copper dots

As discussed in above section, defects might degrade the oxide layer differently. The other possible way to observe this phenomenon is by studying the effect of D-defect size on the copper dots size. D-defects that are present on the wafer surface will be integrated into the oxide layer during thermal oxidation. According to Oka [28], D-defect will degrade the oxide layer during growing of oxide layer. These

defects become the weak spots of the oxide layer. As a result, larger D-defects might have higher chances to degrade the oxide more severely and become the weaker spots of the oxide layer. When these defects are subjected to constant field, the weaker spots might experience more severe breakdown and allow higher magnitude of current to pass through. Since more charges are supplied to the breakdown spots, larger copper dots will be formed on the wafer surface.

To verify above hypothesis, the wafers are copper decorated at applied field of 5±0.5 MV/cm. This is because most of the defects detected at this applied field are D-defects [10-26]. The size of copper dots on wafer surface can be known by using image analyzing system (Carl Zeiss, KS 400). This is followed by recording down the coordinates (location) of these copper dots by using AFM system . Next, the copper dots and oxide layer is removed by using diluted nitric acid (≈ 1% vol., 1 minute) and HF solution (≈ 1% vol, 5 minutes), respectively. Finally, with the help of coordinates of the location of copper dots, AFM is able to measure the size of D-defect found under the copper dots as shown in Figure 4.9 (a), (b), (c) and (d).

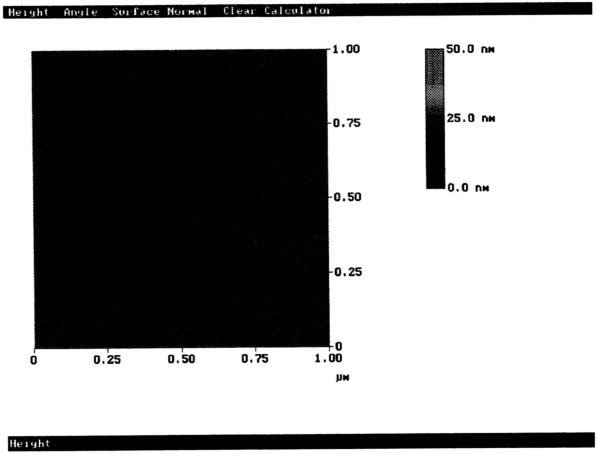

Figure 4.9: (a) D-defect measured by AFM. It is located right at the bottom of copper dot. The scanning size is 1 μm with scan rate 1 Hz. The area of D-defect measured by image analyzing software is 13,882 nm^2.

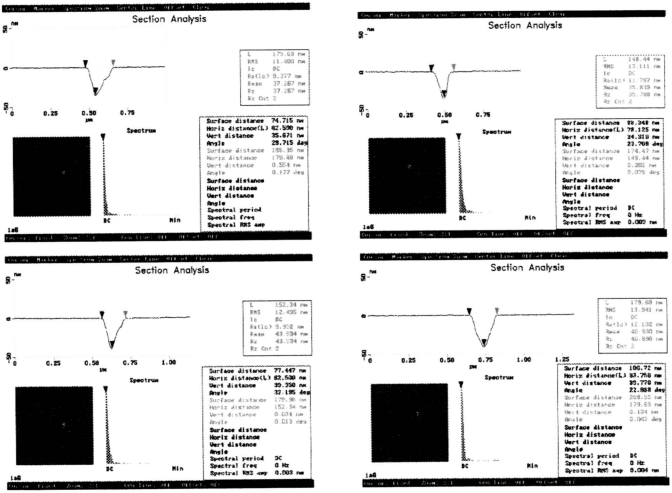

Figure 4.9: (b) The cross section of this D-defect is measured. The average depth and width of the D-defect is 37.28 μm and 165.04 μm, respectively.

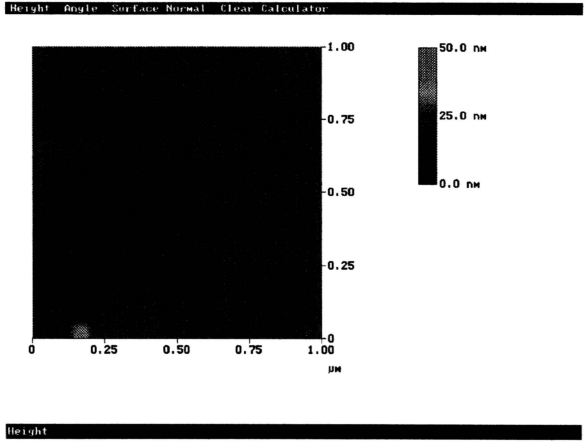

Figure 4.9: (c) Another D-defect detected by AFM. It is located right at the bottom of copper dot. The scanning size is 1 μm with scan rate 1 Hz. The area of D-defect measured by image analyzing software is 15,671 nm^2.

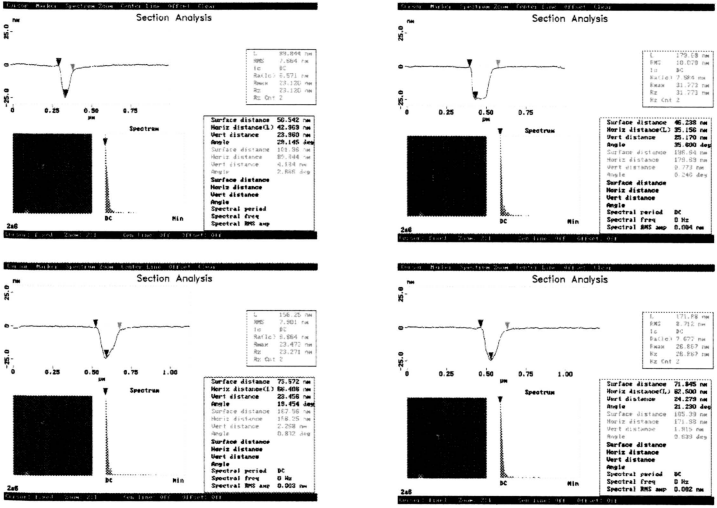

Figure 4.9: (d) The cross section of this D-defect is measured. The average depth and width of the D-defect is 24.22 μm and 149.17 μm, respectively.

The relationship between the size (area) of copper dots and D-defects is then plotted in a graph as given in Fig. 4.10. The results do not show clear relationship between the area of copper dots and area of D-defects. The copper dots size (area) varied from 50,000 –90,000 μm^2 although the area of D-defects was increased from 10,000 to 90,000 nm^2. This give us a hint that the breakdown severity of oxide is determined by the weakest spots of the oxide, rather the size of the D-defects. On the other hand, the relationship between the volume of copper dots and size (area) of D-defects was not studied in this project due to limitation of measurement technique.

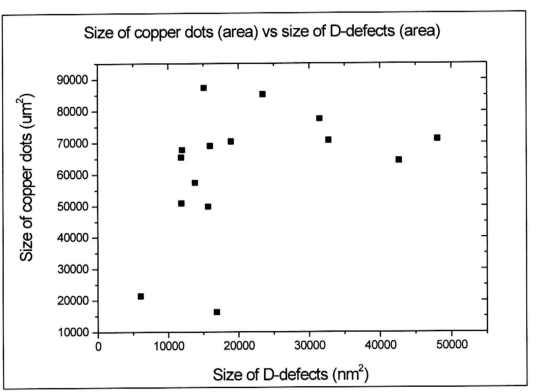

Figure 4.10: No clear relationship between area of copper dots and area of D-defects was observed in this test.

4.1.7 Effect of stressed field on defect density of copper decorated wafers

The other evident can prove that defects in oxide layer degrade oxide differently is by studying the defect density of copper decorated wafers as a function of applied field. Figure 4.11 (a) and (b) show the defect density of copper decorated wafers when a wide range of applied field is applied to stress the oxide layer. The results indicate that the defect density of copper decorated wafers increased with stressed field.

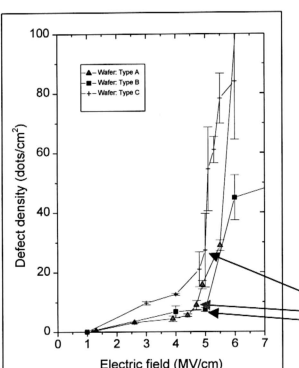

Figure 4.11 (a): Defect density is increased as a function of electric field for different crystals. For all three types of wafers, the defect densities increase substantially when the applied field exceeds the "knee" region.

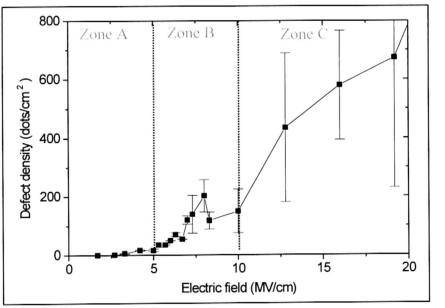

Figure 4.11 (b): Defect density as a function of electric field. Three regions corresponding with different magnitudes of defect densities are observed. In zone A (E < 5MV/cm), the defect density of copper decorated wafers ≤ 20 dots/cm^2. In zone B (5 MV/cm < E < 10MV/cm), the defect density is in the range of 20 ≤ DD ≤ 200 dots/cm^2. High density of copper dots (> 1200 dots/cm^2) is observed in zone C (E > 10MV/cm).

Three regions corresponding with different magnitudes of defect densities are observed. In zone A (E < 5MV/cm), the defect density of copper decorated wafers ≤ 20 dots/cm^2. On the other hand, the defect density is in the range of 20 ≤ DD ≤ 200 dots/cm^2 in zone B (5 MV/cm < E < 10MV/cm). High density of copper dots (> 1200 dots/cm^2) is observed in zone C when applied field greater than 10MV/cm is used. The defect density in this range has shown the tendency of saturation. This observation indicates that the intrinsic breakdown of silicon oxide has been occurred. In fact, literature study [4] has pointed out that the intrinsic breakdown field (E_{bd}) of thermally grown silicon oxide is around 10 MV/cm.

Increasing of defect density as a function of applied field once again indicates that defects degrade the oxide layer differently. When higher stress field is applied to the oxide layer, more breakdown spots are generated through the oxide layer. This results more copper dots grown on the wafer surface.

4.1.8 Analyzing composition of grey ring surrounded copper dots by using TOF-SIMS

When a low magnification of optical microscope (50X) is used to observe the copper dots, it is found that each dots is surrounded by a grey ring (Fig. 4.12). TOF-SIMS is used to identify the composition of the grey ring. The analysis is started with locating the extra or stronger peaks between the copper dot and reference area on the same piece of wafer using secondary ion mass spectra. This information will then be used to carry out secondary ion imaging measurement. This type of measurement allows us to observe the distribution of elements/composition on the copper dot surface.

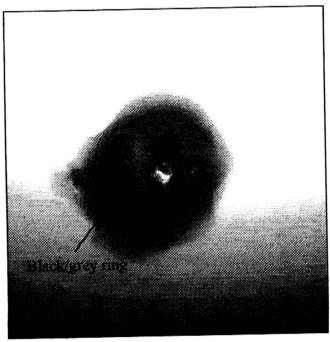

Figure 4.12: The above copper dot has been analyzed by TOF-SIMS to obtain positive secondary ion mass spectra (Scanning area: 500 x 500 μm^2; mass spectra range: 0-500; sampling time: 500 s.)

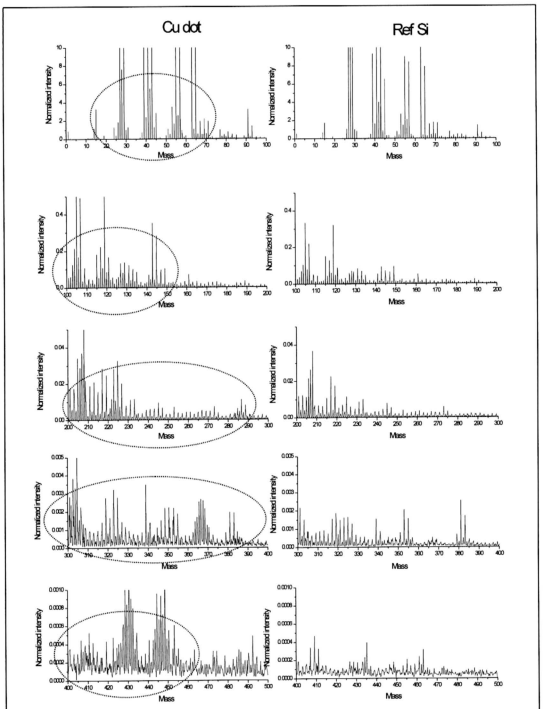

Figure 4.13: Comparison of positively secondary ion mass spectra on copper dot and reference area. Extra and stronger peaks on the copper dot mass spectra compared to reference area are registered. These mass spectra will be measured during measurement of secondary ion mass imaging.

The comparison of these two spectra is shown in Fig. 4.13. There are 41 extra/ stronger peaks on the copper dot mass spectra compared to reference area are identified. They are registered and used during measurement of secondary ion mass imaging. Fig. 4.14 (a) and (b) show both secondary ion mass imaging of reference area and copper dot.

The ion mass imaging on reference area (Fig. 4.14 (a)) detected high intensity of ^{28}Si, ^{30}Si, ^{63}Cu, ^{65}Cu, CH_4Al, CH_3, CH_2 and CH. These compounds are quite evenly distributed on the wafer surface. The source of ^{63}Cu and ^{65}Cu came from copper plate. Organic fragments such as CH_4Al, CH_3, CH_2 and CH are originated from methanol (CH_3OH) itself.

Ion mass imaging on copper dots shows more interesting result (Fig. 4.14 (b)). Basically, one can category the secondary ion imaging into 3 regions, i.e. elements found only (i) at the copper dot region, (ii) at the ring region and (iii) outside the copper dot region.

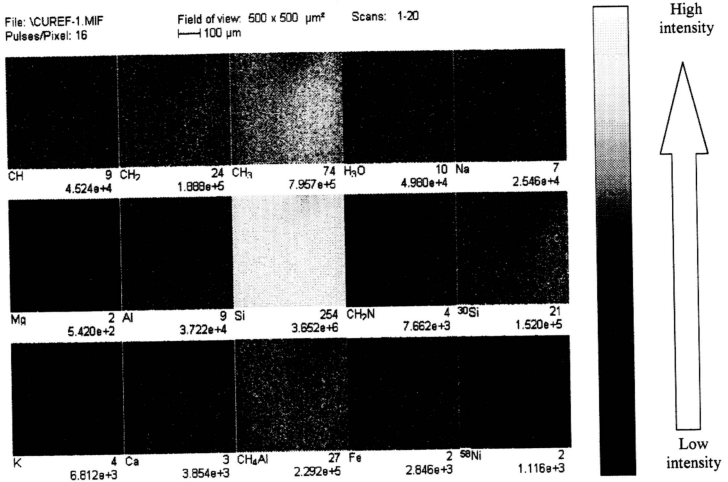

Figure 4.14 (a) (i) Secondary ion mass imaging on reference area. High intensity of ^{28}Si, ^{30}Si, ^{63}Cu, ^{65}Cu, CH_4Al, CH_3, CH_2 and CH are detected.

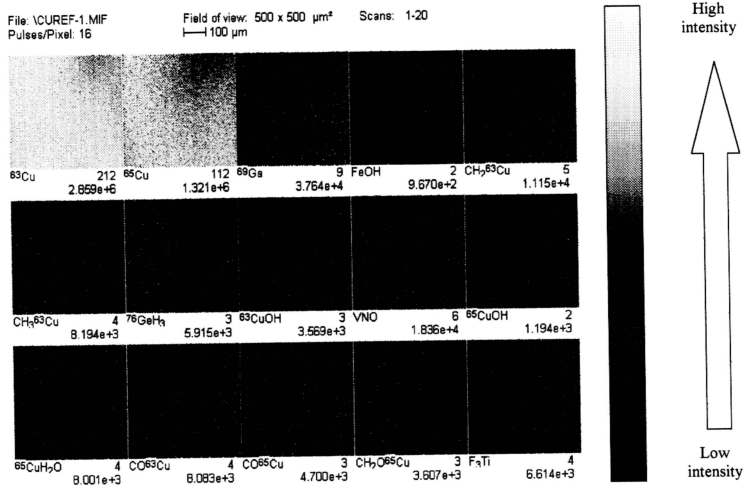

Figure 4.14 (a) (ii) Secondary ion mass imaging on reference area. High intensity of ^{28}Si, ^{30}Si, ^{63}Cu, ^{65}Cu, CH_4Al, CH_3, CH_2 and CH are detected.

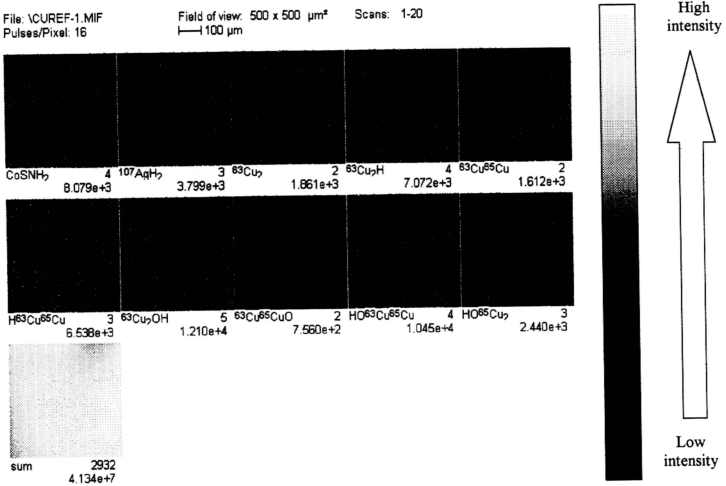

Figure 4.14 (a) (iii) Secondary ion mass imaging on reference area. High intensity of ^{28}Si, ^{30}Si, ^{63}Cu, ^{65}Cu, CH_4Al, CH_3, CH_2 and CH are detected.

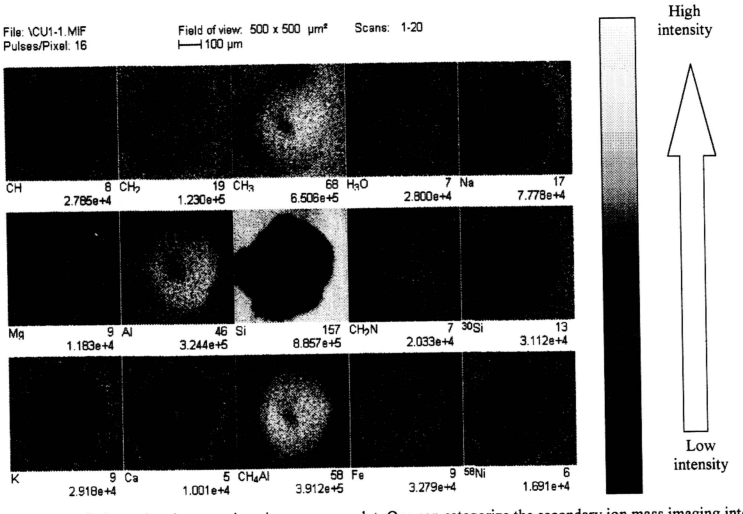

Figure 4.14 (b) (i) Secondary ion mass imaging on copper dot. One can categorize the secondary ion mass imaging into 3 regions, i.e. elements found only (1) at the copper dot region, (2) at the ring region and (3) outside the copper dot region.

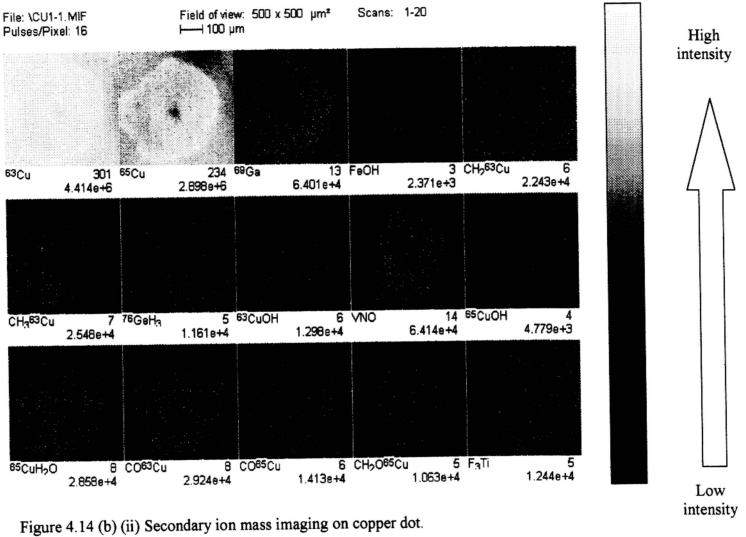

Figure 4.14 (b) (ii) Secondary ion mass imaging on copper dot.

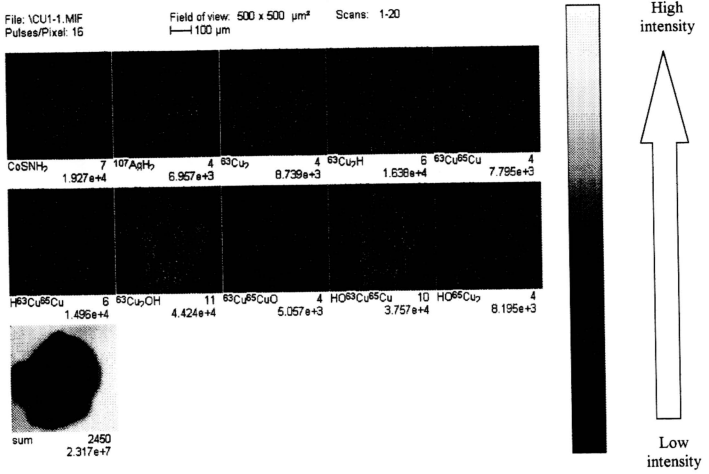

Figure 4.14 (b) (iii) Secondary ion mass imaging on copper dot.

(i) at the copper dot region

Metallic elements/compounds like ^{63}Cu, ^{65}Cu, *Al, Fe, Ga* and *VNO* with high counts are found at the copper dot region. There is no doubt that most of the *Cu* atoms are from the copper plate. Sources of *Al, Fe, Ga* and *VNO* are most likely from methanol. This is because the methanol used consists of these metallic elements with concentration in ppb level (refers to certificate of analysis on methanol at appendix II). This metallic elements deposited on the copper dot region during copper decoration process. Besides, some organo-metallic compounds are also found in this region. The compounds are CH_3, CH_4Al, $^{63}CuOH$, $^{65}CuH_2O$, $CO^{63}Cu$, $CH_2O^{65}Cu$, $^{63}Cu_2OH$ and $HO^{63}Cu^{65}Cu$. The main source of organic compound, especially CH^{3+} is from methanol (CH_3OH).

(ii) at the ring region

High intensity of metallic elements such as *Na, Mg, K and Ca* are found in this region. Human can introduce *Na* easily during carrying out the copper decoration or TOF-SIMS analysis. The remaining metallic elements have very high chances originated from methanol itself.

(iii) outside the copper dot region

Only two elements, i.e, *Si and Ni* show significant high intensity outside the copper dot region. Of course, the source of *Si* is come from the silicon wafer. The *Ni* element is believed to be came from the methanol used during decoration process.

From above analysis, we know that not only copper ions are deposited, but other cations such as *Al, Fe, VNO, CH_3 (fragment), CH_4Al (fragment), $^{63}CuOH$ (fragment), $^{65}CuH_2O$ (fragment), $CO^{63}Cu$ (fragment), $CH_2O^{65}Cu$(fragment), $^{63}Cu_2OH$ (fragment)* and *$HO^{63}Cu^{65}Cu$ (fragment)* are also discharged on the surface. In addition, the result shows that metallic elements such as *Na, Mg, K* and *Ca* are responsible for the black/grey ring formation.

4.1.9 Formation of copper dots on copper decorated wafer

The sources of defects present on a piece of wafer can originate from crystal grown-in defects such as D-defects, oxygen precipitates and stacking faults. Defects can also be introduced on the wafer during process for examples, metallic contamination, scratches and particles. When a wafer is sent for oxidation, oxide layers will grow on the wafer surface. The oxide layers not only grow on top of the wafer but also eat into the wafer surface. According to the model proposed by Deal and Grove [6, 8], 44.5% of the oxide thickness is contributed by the silicon wafer. Defects, which are present on the wafer surface before oxidation, will be integrated into oxide layer during oxidation. As a result, these defects become the weak spots in the oxide layer.

Weak spots in the oxide layer are not able to withstand high stress field. Depending on the degradation introduced by the defects on the oxide layer, these weak spots will experience low-field breakdown, or defect related breakdown when they are stressed by applied field. When oxide breakdown occurs, localized conducting paths (permanent damages) not only propagate through the oxide layer (insulator), they also extend to the wafer surface. This allows high magnitude of current density to flow through the breakdown spot. It is believed that the magnitude of current flowing through the breakdown spots depends on the damages done on the oxide layer during oxide breakdown. The electrical current flowing through the oxide layer supplies the electric charges that is needed to discharge cations (especially copper ions) at the cathode. As a result of different magnitude of

current flow through the breakdown spots, the copper dots form on the wafer surface exhibit a wide range of size distribution.

From TOF-SIMS analysis, not only Cu^{2+} ions are attracted, discharged and deposited as copper dots on oxide surface, other cations such as *Al, Fe,* CH_3^+, CH_4, $^{63}Cu^{2+}$, $^{65}Cu^{2+}$, *and* CH_2^{2+}, compete with each other to deposit on oxide surface. These copper dots therefore are formed right on top of the defects in the oxide layer. A possible mechanism for copper dots formation on oxide surface is illustrated in Fig. 4.15 (a), (b) and (c).

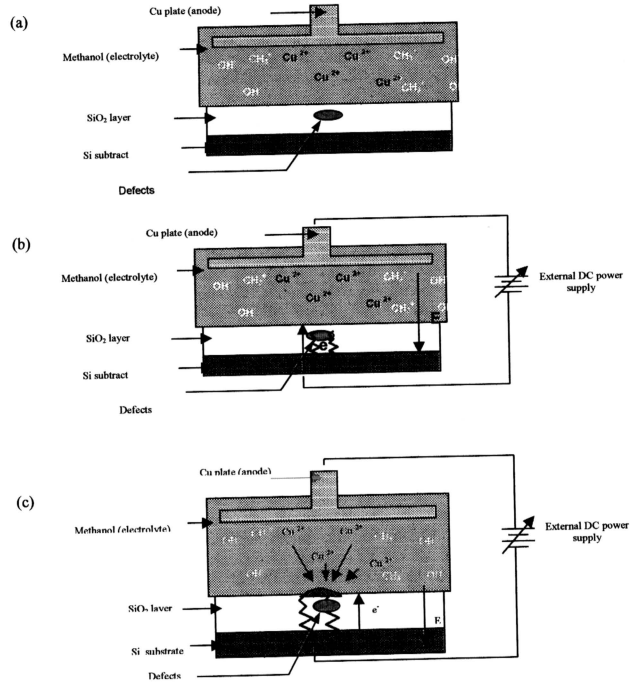

Figure 4.15 : (a) Oxidized wafer consists of defects in oxide layer is loaded into the copper decoration equipment. The defects are weak spots in the oxide layer. The wafer is then immersed into methanol, which acts as electrolyte in this case. (b) When the oxide layer is subjected to electric field, oxide breakdown occurs on these weak spots. Localized conducting path is generated, allowing current to flow through the oxide layer. (c) Cations especially copper ions are attracted, discharged and deposited on oxide surface as copper dot.

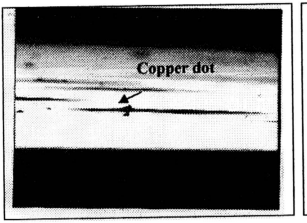

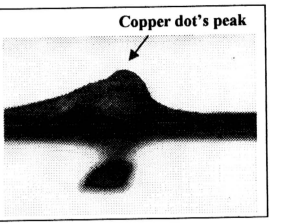

Figure 4.16 (a): The image of the copper dots captured by SEM at an angle of 45° to the wafer surface (magnification: 50X). (b): A peak is observed on the copper dot. This image is captured at a magnification of 2000X with the electron beam almost parallel to the wafer surface.

Fig. 4.16 shows SEM images of copper dots viewed at different angles and magnifications. A peak is observed on the copper dot. A model is proposed to explain the presence of the peak on the copper dot. Since the formation of dots is due to discharge of copper ions, the amount of copper ions deposited should depend on the current and discharging time. Consequently, the existence of the peak on the copper dot might be due to the following reasons:

(i) The oxide underneath the copper peak is the origin of a localized breakdown spot. Therefore, the spot allows longer deposition time of copper ions (Fig. 4.17 (a)),

(ii) The oxide underneath the copper peak experienced the most severe breakdown, allowing higher current density to flow through (Fig. 4.17 (b)), or

(iii) A combination of model (i) and (ii).

Since formation of copper dots involves the electrolysis process, model (iii) is the most probable mechanism of copper dots formation.

(a) model (i)

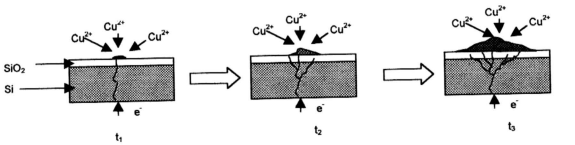

(b) model (ii)

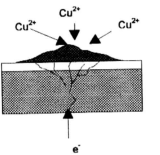

Figure 4.17: The presence of a peak at the copper dot can be due to (i) the oxide underneath the peak experiencing longer deposition time since it is the origin of breakdown spot, or (ii) the oxide underneath the peak experiencing the most severe breakdown, therefore high current density is conducted through the region, or (iii) the combination of (i) and (ii).

4.2 Determination of stressed field by V_{ox} / V_{app} ratio measurement

As discussed in section 4.1.7, the magnitude of stressed field (or V_{ox}) will determine the defect density of copper decorated wafers. Therefore, it is important to know the actual voltage used to stress the oxide layer. However, due to the gap between anode and cathode of the copper decoration unit, there is a voltage drop (V_{drop}) across the methanol. The voltage used to stress the oxide layer (V_{ox}) is smaller than the applied voltage (V_{app}) as illustrated in Fig. 4.18.

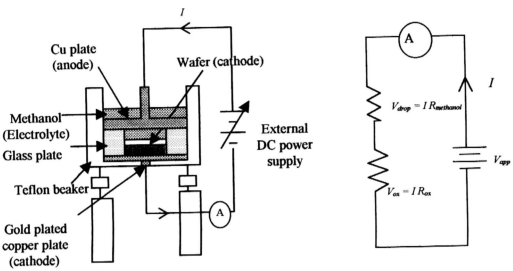

Figure 4.18: Schematic diagram of copper decoration apparatus. There is a gap (≈ 0.5cm) between the anode and the cathode. As a result, there is a voltage drop across the gap that is filled with methanol. The voltage relationship is given by $V_{ox} = V_{app} - V_{drop}$.

Normally, a V_{ox} /V_{app} ratio measurement is carried out to determine the stressed field as given in equation (14), section 3.2.3. In this measurement, it is found that the V_{ox}/V_{app} ratio is dependent on the exposed test probe length.

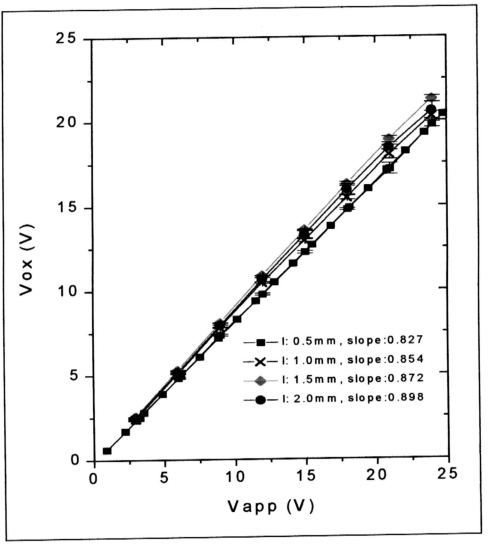

Figure 4.19: V_{ox} as a function of V_{app} with different exposed test probe length s(Diameter: 0.56mm). The V_{ox}/V_{app} ratios (slopes) increase with longer test probes

Fig. 4.19 shows the results for the V_{ox} measurement as a function of V_{app} with different exposed voltage probe lengths. The results indicate that the relationship between V_{ox} and V_{app} for exposed probe length up to 2.0 mm is linear. The V_{ox}/V_{app} ratios increase with longer exposed probe lengths. Since the resistivity of the electrolyte (methanol) is relatively high, the exposed wire provides a shorter

a shorter path for the current (or charge carriers) in the vicinity of the probe. This leads to voltage measurement that is dependent on the exposed lengths.

In an ideal case, we would like to eliminate the effects of the exposed probe length on the V_{ox} measurement. This can be achieved if the exposed length is close to zero. However in practice, this poses some difficulty in the experimental measurement because the probe needs to make contact with the wafer surface. Due to these difficulties, we propose that the value for the V_{ox} / V_{app} ratio used in the calculation of the stress field is obtained by extrapolating the V_{ox} / V_{app} to zero exposed probe length, as shown in Fig. 4.20. In this case, the V_{ox} / V_{app} ratio determined on the wafer surface is 0.802. This means that if V_{app} is 15V, the V_{ox} will be 12.03V and V_{drop} is 2.97V.

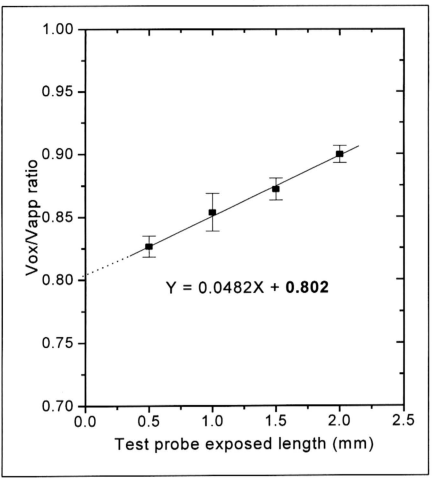

Figure 4.20: The V_{ox}/V_{app} ratios obtained from Fig. 4.18 are plotted as a function of test probe exposed length. By extrapolating the test probe length to zero, one can determine a better accuracy of V_{ox}/V_{app} ratio.

4.3 Effects of copper concentration in methanol on copper decoration process

From the previous findings in section 4.1, we know that electrolysis process occurs during copper decoration process. As a result, copper concentration in methanol is building up during the process. Effects of copper concentration in methanol on conductivity of methanol and the size of copper dots will be discussed in the following section.

4.3.1 Effects of copper concentration on the conductivity of methanol

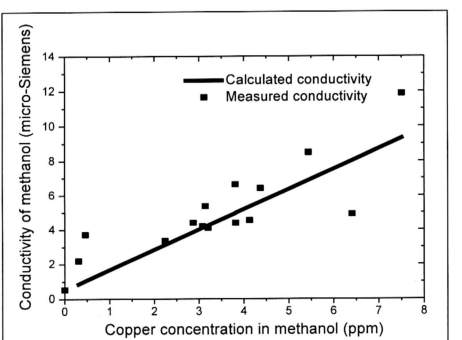

Figure 4.21: The conductivity of methanol increases with copper concentration in methanol. It is found that the measured conductivity is correlated well with the calculated conductivity. Consequently, it is reasonable to assume that copper ions are the main current in methanol and contribute to the conductivity of methanol.

As illustrated in Fig. 4.21, the experiment result indicates that the conductivity of methanol increases linearly with copper concentration in methanol with $r^2 = 0.7105$. This result is used to compare with calculated value. The conductivity of methanol as a function of copper concentration can be estimated by slight modification of equation (8) in section 2.1.3.2.

$$k_i = \left(\frac{e^2 N_A}{6\pi\eta}\right)\left(\frac{z_i^2}{r_i}\right)c_i \qquad (8)$$

Two assumptions have been made to simplify the calculation.

(i) The viscosity of methanol (η) does not change with time. It is given as $\eta = 5.86 \times 10^{-4}$ kg/ s m at 20^0C [74].

(ii) Charge conduction in methanol is related to conductivity of methanol. The main ions responsible for charge conduction in methanol is assumed to be copper ions. Charge conduction due to other ions is assumed to be negligible.

Since the main ions responsible for charge transportation is assumed to be copper ions, one can fix (z_i^2 / r_i) as a constant. Therefore, equation (8) can be simplified as

$$k = \left(\frac{e^2 z^2 N_A}{6\pi\eta r}\right)c_i$$

$$k = B\,[Cu^{2+}] \qquad (17)$$

where charge of electron, $e = 1.6 \times 10^{-19}$ C, oxidation number of copper ions, $z = 2$, Avorgado number, $N_A = 6.023 \times 10^{-23}$ (mol^{-1}), viscosity of methanol, $\eta = 5.86 \times 10^{-4}$ kg/s m at 20°C [74], radius of copper ions, $r = 0.75 \times 10^{-10}$ m [51] and copper concentration in methanol (mol/ m^3), $c_i = [Cu^{2+}]$.

B is a constant number,

$$B = \left(\frac{e^2 z^2 N_A}{6\pi\eta r} \right)$$

$$= 0.07445 \ (A^2 \ s^3 / \text{mol kg})$$

In practice, the initial conductivity of methanol is given as $k_O = 0.5$ μS. Equation *(17)* can be modified again as

$$k = B[Cu^{2+}] + k_O$$

$$\text{or } k \ (\mu S) = 0.07445[Cu^{2+}] + 0.5 \qquad (18)$$

Equation *(18)* shows that the conductivity of a methanol (k) is proportional to the concentration of copper ions ($[Cu^{2+}]$) in the solution. This is because copper ions are available for charge transportation from anode to cathode. The conductivity of methanol with different copper concentration is calculated using equation *(18)*. This calculated conductivity is agrees well with the experimental value as shown in Fig. 4.21. The good correlation between copper concentration and conductivity of methanol can be used for real time monitoring of the copper concentration in

methanol.

4.3.2 Effects of copper concentration on the size (average diameter) of copper dots

The relationship between copper concentration in methanol with average diameter of copper dots is studied. The measurement of the average diameter of copper dots is as illustrated in Fig. 3.11 As shown in Fig. 4.22, the average size of the copper dots deposited on the wafer increases with copper concentration in methanol.

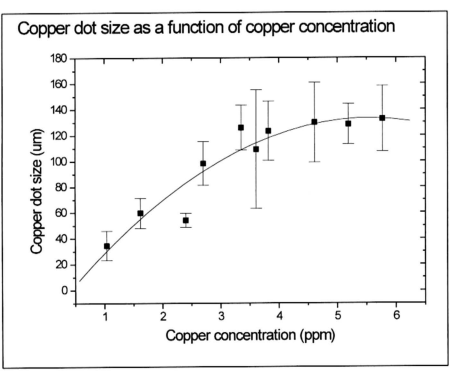

Figure 4.22: Larger copper dots can be obtained at higher copper concentration in methanol. (Each data points is the average size of copper dots from 3 pieces of wafers, 5 random copper dots per piece of wafers. Besides, the deposition time for each wafers is 5 minutes.)